Tectonophysics 679 (2016) 235–245

Contents lists available at ScienceDirect

Tectonophysics

journal homepage: www.elsevier.com/locate/tecto

The deep structure of south-central Taiwan illuminated by seismic tomography and earthquake hypocenter data

Giovanni Camanni [a,*], Joaquina Alvarez-Marron [a], Dennis Brown [a], Concepcion Ayala [a,1], Yih-Min Wu [b], Hsien-Hsiang Hsieh [c]

[a] Institute of Earth Sciences Jaume Almera, ICTJA–CSIC, Lluis Sole i Sabaris s/n, 08028 Barcelona, Spain
[b] Department of Geosciences, National Taiwan University, Taipei 106, Taiwan
[c] Institute of Oceanography, National Taiwan University, Taipei 106, Taiwan

ARTICLE INFO

Article history:
Received 15 January 2015
Received in revised form 11 June 2015
Accepted 20 September 2015
Available online 30 September 2015

Keywords:
Basement-cover interface
Detachment
Basement involvement
Structural inheritance
Taiwan
Earthquake seismicity

ABSTRACT

The Taiwan mountain belt is generally thought to develop above a through-going basal thrust confined to within the sedimentary cover of the Eurasian continental margin. Surface geology, magnetotelluric, earthquake hypocenter, and seismic tomography data suggest, however, that crustal levels below this basal thrust are also currently being involved in the deformation. Here, we combine seismic tomography and earthquake hypocenter data to investigate the deformation that is taking place at depth beneath south-central Taiwan. In this paper, we define the basement as any pre-Eocene rifting rocks, and use a P-wave velocity of 5.2 km/s as a reference for the interface between these rocks and their sedimentary cover. We found that beneath the Coastal Plain and the Western Foothills clustering of hypocenters near the basement-cover interface suggests that this interface is acting as a detachment. This detachment is located below the basal thrust proposed from surface geology for this part of the mountain belt. Inherited basement faults appear to determine the geometry of this detachment, and their inversion in the Alishan area result in the development of a basement uplift and a lateral structure in the thrust system above them. However, across the Shuilikeng and the Chaochou faults, earthquake hypocenters define steeply dipping clusters that extend to greater than 20 km depth, above which higher velocity basement rocks are uplifted beneath the Hsuehshan and Central ranges. We interpret these clusters to form a deeply penetrating, east-dipping ramp that joins westward with the detachment at the basement-cover interface. It is not possible to define a basal thrust to the east, beneath the Central Range.

1. Introduction

The Taiwan mountain belt has been forming since the Late Miocene as a result of the oblique collision between the southeast continental margin of Eurasia and the Luzon volcanic arc on the Philippine Sea Plate (Byrne et al., 2011; Huang et al., 2006; Lin et al., 2003; Mesalles et al., 2014; Sibuet and Hsu, 2004; Suppe, 1981, 1984; Teng, 1990) (Fig. 1). Studies of the structure of the western flank of the Taiwan mountain belt have led many authors to suggest that it is evolving by thrusting above a shallowly east-dipping basal thrust that extends all the way eastward beneath the orogen (Carena et al., 2002; Ding et al., 2001; Malavieille and Trullenque, 2009; Suppe, 1980, 1981; Suppe and Namson, 1979; Yue et al., 2005). Although both along- and across-strike variations in the depth and stratigraphic location of the basal thrust have been proposed, it is generally thought to be confined to within the sedimentary cover of the margin, either at the base of the syn-orogenic sediments or within the older pre-orogenic platform and slope sediments (Brown et al., 2012; Suppe, 1976, 1980, 1981; Suppe and Namson, 1979; Yue et al., 2005).

There are, however, a number of pieces of evidence in the surface geology (Alvarez-Marron et al., 2014; Brown et al., 2012; Camanni et al., 2014a), as well as in magnetotelluric (Bertrand et al., 2009, 2012), GPS (Chuang et al., 2013), earthquake hypocenter (Gourley et al., 2007; Lacombe and Mouthereau, 2002; Lacombe et al., 2001; Mouthereau and Petit, 2003; Wu et al., 1997, 2004, 2008, 2014; Yue et al., 2005) and seismic tomography data (Alvarez-Marron et al., 2014; Camanni et al., 2014b; Huang et al., 2014; Kim et al., 2005, 2010; Kuo-Chen et al., 2012; Lin, 2007; Rau and Wu, 1995; Wu et al., 2007) which suggest that rocks below the interpreted basal thrust, and even the basement (here, according to Ho(1986, 1988), we define basement as any pre-Eocene rifting rocks, but it is often defined by others as any pre-Miocene rocks) may also be involved in the deformation in much of Taiwan. For example, combining surface geological and borehole data,

* Corresponding author at: Fault Analysis Group, School of Geological Sciences, University College Dublin, Belfield Dublin 4, Ireland.
E-mail addresses: giovanni.camanni@ucd.ie (G. Camanni), jalvarez@ictja.csic.es (J. Alvarez-Marron), dbrown@ictja.csic.es (D. Brown), cayala@ictja.csic.es (C. Ayala), drymwu@ntu.edu.tw (Y.-M. Wu), denny.hsieh@gmail.com (H.-H. Hsieh).
[1] Permanent address: Instituto Geológico y Minero de España — IGME (Spanish Geological Survey), La Calera n. 1, 28760 Tres Cantos, Madrid, Spain.

http://dx.doi.org/10.1016/j.tecto.2015.09.016
0040-1951/

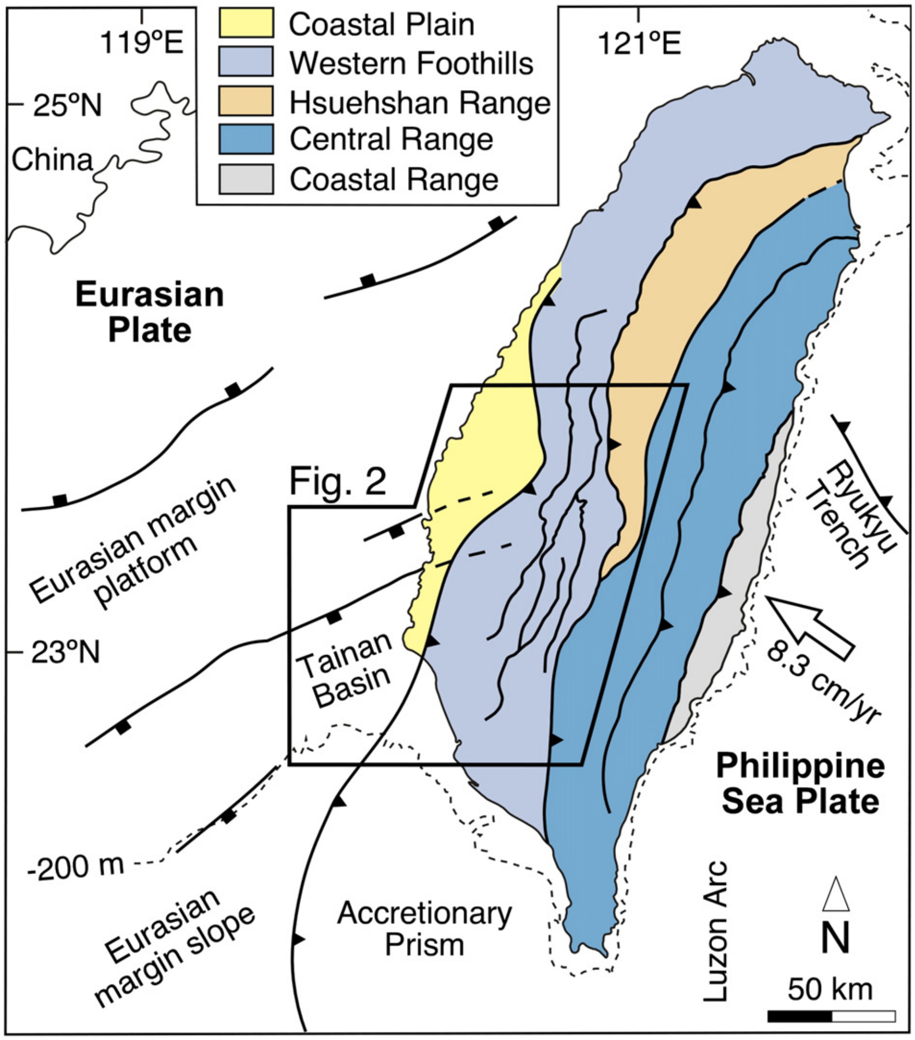

Fig. 1. Tectonic setting and major tectonostratigraphic zones of the Taiwan mountain belt. The −200 m isobath marks the current location of the shelf-slope break in the Eurasian margin. The structures on the Eurasian margin and the location of the deformation front offshore southwestern Taiwan are from Lin et al. (2008), Lin et al. (2003), Shyu et al. (2005), and Yeh et al. (2012). The location of Fig. 2 is shown.

Hickman et al. (2002) and Hung et al. (1999) interpret the basal thrust to cut down section to lie near the basement-cover interface. Similarly, seismic activity beneath the interpreted location of the basal thrust in west-central and southwestern Taiwan also led Mouthereau and Petit (2003) and Yue et al. (2005) to postulate the presence of a second, deeper detachment surface that lies either near the basement-cover interface or within the basement. Furthermore, on the basis of surface geological, borehole and seismicity data, Mouthereau et al. (2001, 2002), Lacombe and Mouthereau (2002), and Mouthereau and Lacombe (2006), interpret the basement (note that they call basement any pre-Miocene rocks) to be involved in the deformation along much of westernmost Taiwan. Eastward, Brown et al. (2012), Camanni et al. (2014a, b), and Chuang et al. (2013) use either surface geology, seismicity, or GPS data to interpret the basal thrust to ramp down into the middle crust and to involve basement in the deformation. These latter observations are further corroborated by the presence of high P-wave velocities (up to 5.5 km/s) close to the surface, suggesting that basement rocks are being uplifted (e.g., Alvarez-Marron et al., 2014; Camanni et al., 2014b; Huang et al., 2014; Kim et al., 2005, 2010; Kuo-Chen et al., 2012; Lin, 2007; Rau and Wu, 1995; Wu et al., 2007). Furthermore, in much of Taiwan Wu et al. (1997, 2004, 2014) and Gourley et al. (2007) have used earthquake hypocenter data to suggest that there are a number of steeply dipping faults that penetrate into the middle and perhaps even the lower crust.

These observations suggest that deformation that is taking place near the basement-cover interface and within the basement may be playing a more significant role in the structural development of the Taiwan orogeny than predicted by the model with a basal thrust confined to within the sedimentary cover. To help place further constraints on the structural architecture of the Taiwan mountain belt, in this paper we use a P-wave tomography model to define a proxy for the basement-cover interface in south-central Taiwan (Figs. 1 and 2). We then use earthquake hypocenter data to evaluate the location and the geometry of deep-seated faults that are contributing to the deformation that is taking place in this part of Taiwan.

2. Geological setting

The outcropping geology of the south-central part of the Taiwan mountain belt (Figs. 1 and 2) is made up of Eocene to Miocene sediments of the continental margin overlain by Pliocene to Holocene synorogenic sediments of the foreland basin (Brown et al., 2012; Hickman et al., 2002; Hung et al., 1999; Lacombe et al., 1999; Mouthereau et al., 2001; Rodriguez-Roa and Wiltschko, 2010; Yue et al., 2005). Basement

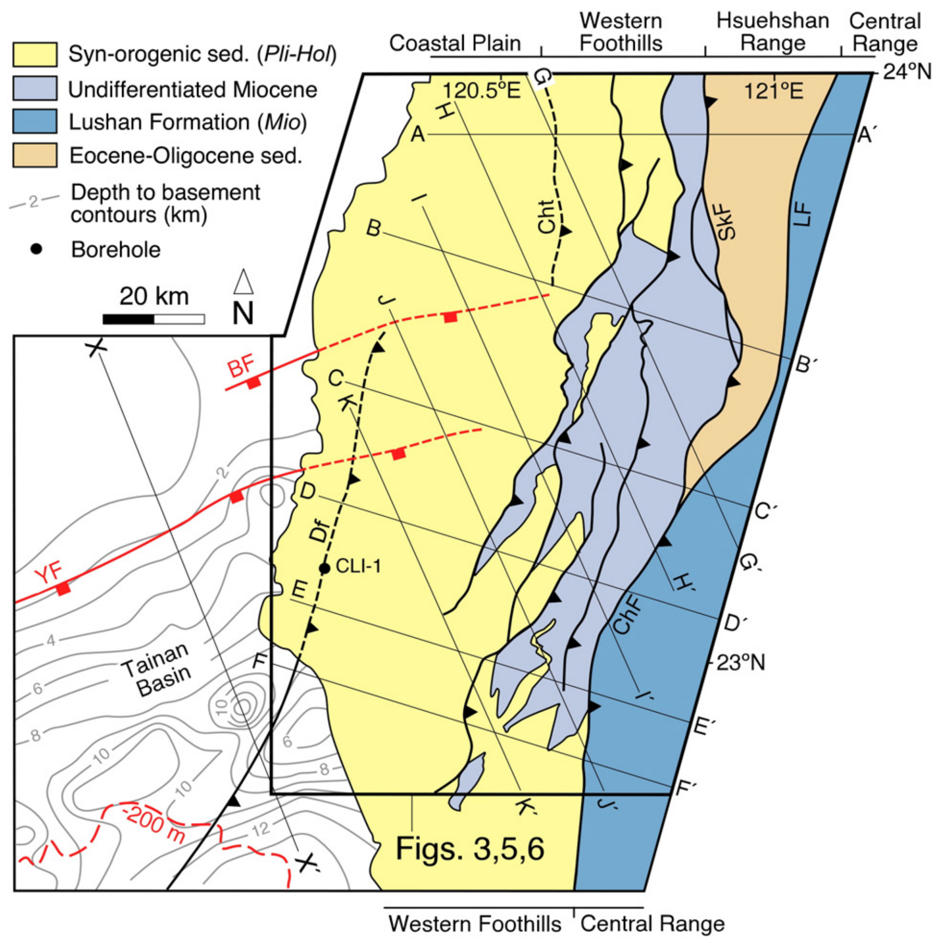

Fig. 2. Major geological features of the study area. Fault traces are from our own field data with the exception of the deformation front in the southwestern part of the study area, which is from Shyu et al. (2005). The structure offshore south-central Taiwan is from Lin et al. (2003), as are the contours representing the top of the basement. The location of the borehole discussed in the text is shown, as is the location of Figs. 3, 5, and 6. Fault abbreviations: BF, "B" Fault; ChF, Chaochou Fault; ChT, Changhua Thrust; Df, Deformation front; LF, Lishan Fault; SkF, Shuilikeng Fault; YF, Yichu Fault.

rocks do not crop out within the study area, although they have been intersected in a number of boreholes (Chiu, 1975; Jahn et al., 1992; Mouthereau et al., 2002; Shaw, 1996). This basement predominantly comprises clastic sediments of Jurassic and Cretaceous age (Chiu, 1975; Shaw, 1996), although there is some dispute as to the correctness of these ages (e.g., Chiu, 1975). Only in one borehole in the southern part of the study area (CLI-1, Fig. 2) has marble been found, from which a Pb–Pb isochron age of 242 ± 22 Ma, or Triassic, has been determined (Jahn et al., 1992).

In this part of Taiwan, the mountain belt can be roughly divided into four tectonostratigraphic zones separated by major faults (Figs. 1 and 2). From west to east these zones are: the Coastal Plain, the Western Foothills, the Hsuehshan Range, and the Central Range. The Coastal Plain is made up of weakly deformed Pliocene to Holocene syn-orogenic sediments of the foreland basin, while the Western Foothills comprise a west-verging thrust system that imbricates the Miocene pre-orogenic and the younger syn-orogenic sediments (Alvarez-Marron et al., 2014; Brown et al., 2012; Hickman et al., 2002; Hung et al., 1999; Lacombe et al., 1999; Rodriguez-Roa and Wiltschko, 2010; Yue et al., 2005). In much of central and southern Taiwan, the boundary between the Coastal Plain and the Western Foothills is generally interpreted to coincide with the tip line of the Changhua Thrust (Fig. 2), which is usually presented as the deformation front of the Western Foothill thrust system (Ching et al., 2011b; Hsu et al., 2009; Yu et al., 1997). In the southwestern part of the study area, however, on the basis of seismicity, GPS, and geomorphology data, some authors place it farther west (Fig. 2; Lin and Watts, 2002; Shyu et al., 2005; Yang et al., 2007). The Western Foothill thrust system appears to be linked to an east-dipping basal thrust that, in the northernmost part of the map area, is located at the base of the syn-orogenic sediments (Brown et al., 2012; Carena et al., 2002; Mouthereau and Lacombe, 2006; Mouthereau et al., 2002; Suppe, 1981; Yue et al., 2005), while in the central and southern parts it cuts down section into Miocene sediments (Alvarez-Marron et al., 2014; Hickman et al., 2002; Lacombe et al., 1999; Mouthereau and Lacombe, 2006; Mouthereau and Petit, 2003; Mouthereau et al., 2001, 2002; Suppe, 1976; Suppe and Namson, 1979) and, locally, may lie within undifferentiated pre-Miocene rocks (Hickman et al., 2002; Hung et al., 1999).

In the north of the study area, the Western Foothills are juxtaposed against the Hsuehshan Range across the Shuilikeng Fault (Brown et al., 2012; Camanni et al., 2014a) (Fig. 2). The Hsuehshan Range is made up of variably metamorphosed (Beyssac et al., 2007; Sakaguchi et al., 2007; Simoes et al., 2012) Eocene and Oligocene clastic sediments that were deposited in the so-called Hsuehshan Basin (Ho, 1988; Huang et al., 1997; Teng and Lin, 2004). The Hsuehshan Range is juxtaposed against the Central Range in the east across the Lishan Fault (Brown et al., 2012; Camanni et al., 2014b; Clark et al., 1993; Lee et al., 1997). Southward, the Central Range is juxtaposed against the Western Foothills along the Chaochou Fault (Mouthereau et al., 2002; Tang et al., 2011; Wiltschko et al., 2010). The outcropping geology of the Central Range within the study area is made up of Miocene rocks of the Lushan Formation (Beyssac et al., 2007; Brown et al., 2012; Lee et al., 2006; Simoes et al., 2007; Tillman and Byrne, 1995; Wiltschko et al., 2010) which comprises variably metamorphosed slates with a well-developed cleavage (Brown et al., 2012; Fisher et al., 2002; Stanley et al., 1981; Wiltschko et al., 2010).

3. Data and methodologies used

In what follows in Section 4, we use the 3D P-wave velocity model of Wu et al. (2007) in combination with earthquake hypocenter data to investigate the deep structure of south-central Taiwan. The 3D P-wave velocity model is used to determine a proxy for the location and geometry of the basement-cover interface. The reader is referred to Wu et al. (2007) for the data, the methodology used in the tomography inversion, and the resolution testing. Importantly for this study, the horizontal resolution of the model in the study area is 7.5 km in the WNW–ESE direction by 12.5 km in the NNE–SSW direction, whereas the depth resolution is 2 km from 0 to 6 km depth, 3 km from 6 to 9 km depth, 4 km from 9 to 25 km depth, and then 5 km to the base of our data set at 30 km depth.

Earthquake hypocenter data from 1990 to 2011 were first located in the 3D P-wave velocity model using the methodology of Wu et al. (2008). Hypocenters were subsequently collapsed (relocated) using the methodology of Jones and Stewart (1997). Collapsing involves the determination of statistical measurements for standard errors in the depth, latitude and longitude for each event (ERH and ERZ in the database of Wu et al. (2008)) and the clustering of events with overlapping error spheroids. A 3D spatial uncertainty of 4 standard deviations was used to truncate confidence ellipsoid and estimated variance in the data. During this process, hypocenter movements were compared with χ^2 distribution and repeated until a minimum misfit was reached.

In the description of the velocity model that follows in Section 4.2, vertical and horizontal slices were cut through the volume and the collapsed hypocenters were projected on to them. The vertical sections were cut perpendicular to the strike of the surface geological structures and perpendicular to the strike of the extensional fault systems imaged offshore southwest Taiwan and beneath its western Coastal Plain (e.g., Lin et al., 2003). Horizontal slices were cut through the nodal points of the velocity model grid.

Since defining the location and geometry for the top of the basement is of primary importance in this study, we first looked at laboratory measurements carried out on clastic rocks similar to those described as pre-Eocene in boreholes within the study area. These laboratory measurements indicate that weakly metamorphosed polymictic clastic sediments (e.g., dry sandstone) at a depth of between 5 and 15 km, and at temperatures thought to occur at these depths in Taiwan (Wu et al., 2013; Zhou et al., 2003), have a P-wave velocity of ≥5 km/s (Christensen, 1989; Christensen and Stanley, 2003; Johnston and Christensen, 1992, 1993). We therefore chose a P-wave velocity of 5.2 km/s as a velocity description for these rocks, and the 5.2 km/s isovelocity surface as a proxy for the top of the pre-Eocene lithological basement within the study area. We stress, however, that this definition is one of physical properties and it may not coincide with the top of the lithological basement everywhere. In the absence of direct data it nevertheless serves as a marker horizon that helps with the first order interpretation of the crustal structure. Furthermore, tests made using velocities between 5 km/s and 5.5 km/s resulted in isovelocity surfaces that overall show a similar geometry, and plot in a similar location and at a similar depth (see Supplementary Fig. 1). Finally, a velocity of 5.2 km/s for the top of the pre-Eocene basement is also consistent with estimates of Van Avendonk et al. (2014) that interpret the basement to Miocene sediments in the Western Foothills of Taiwan to coincide with a P-wave velocity of 5.0 km/s, and with those of Eakin et al. (2014) who interpret the basement to the platform sediments offshore Taiwan to have a P-wave velocity above 5.0 km/s. It is, however, slightly higher than the c. <5 km/s given to basement by Chen and Yang (1996) and Tang and Zheng (2010).

4. Results

4.1. The basement-cover interface

The basement-cover interface as defined by the 5.2 km/s isovelocity surface (Fig. 3) deepens southward beneath the Coastal Plain and the Western Foothills from c. 8–10 km to c. 15 km, whereas it shallows eastward to less than 4 km depth beneath the Hsuehshan and Central ranges. An exception to this overall trend occurs in the central part of the map area where, immediately to the east of the Changhua thrust, it begins to shallow, defining a basement high that we call the Alishan Uplift (Alvarez-Marron et al., 2014) (AU, Fig. 3). The depth of the basement-cover interface determined in this way is overall deeper than that previously proposed from beneath the Coastal Plain, where its location is derived from borehole and seismic reflection data (Lin et al., 2003). The differences in depth between the two interpretations are on the order of several kilometers (see Supplementary Fig. 2 for comparison and a misfit calculation). These differences can be related to a number of factors, including; 1) the vertical resolution of the P-wave velocity model used here, 2) the depth conversion of time-migrated seismic reflection data by Lin et al. (2003) and, 3) the choice of 5.2 km/s as marking top basement. Mouthereau et al. (2002) also produce a top-basement contour map, but in their case this implies any pre-Miocene rocks so it is not possible to do a direct comparison with our results. Only one borehole (CLI-1, Fig. 2) unequivocally intersects Mesozoic basement in our study area (e.g., Chiu, 1975; Jahn et al., 1992; Shaw, 1996) and its location at −4612 m is significantly deeper than our interpretation. Despite these inconsistencies in the depth between interpretations, the overall geometry of the top of the basement obtained by the 5.2 km/s isovelocity surface, especially its southward deepening, is consistent between models. Note that the interpretation presented here extends into the Western Foothills, Hsuehshan, and Central ranges whereas those of Lin et al. (2003) and Mouthereau et al. (2002) do not.

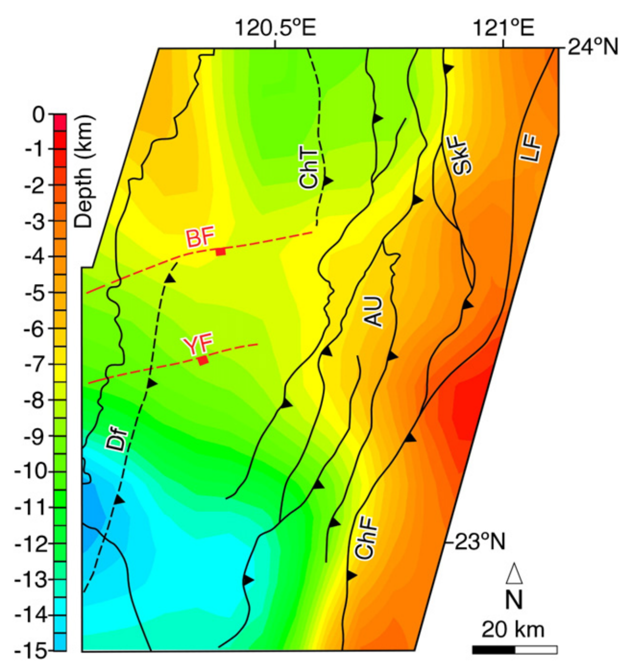

Fig. 3. Depth distribution of the 5.2 km/s isovelocity surface, which we interpreted to be at or near the basement-cover interface. Fault abbreviations are as in Fig. 2. AU, Alishan Uplift. Location of the map is given in Fig. 2.

4.2. The basement-cover interface and earthquake hypocenters

Having established our working definition for the basement-cover interface, its location, depth, and geometry, we now proceed with the descriptions of the velocity and hypocenter data using the 5.2 km/s isovelocity surface as a reference.

In the P-wave velocity sections oriented perpendicular to the strike of the surface structures, the basement-cover interface (the 5.2 km/s isovelocity line) shows a marked shallowing from west to east (Fig. 4A), with the change taking place approximately at the Shuilikeng Fault in the north (sections A-A′, B-B′, and C-C′) and the Chaochou Fault in the south (sections D-D′, E-E′, and F-F′). West of the Shuilikeng and

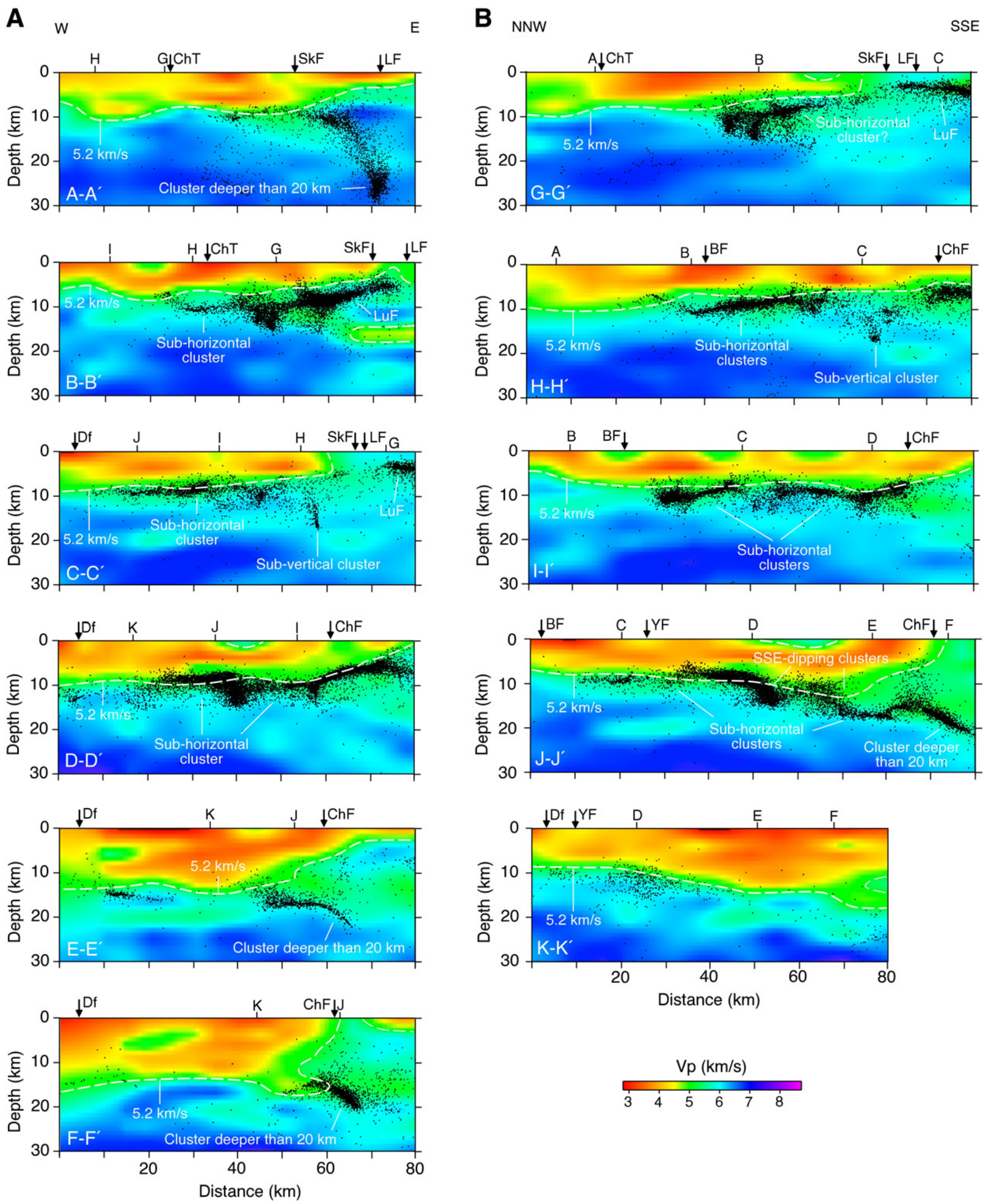

Fig. 4. Vertical sections through the 3D P-wave velocity model (Wu et al., 2007) and the relocated (Wu et al., 2008) and collapsed seismicity dataset. These sections are (A) orthogonal to the structural grain of the mountain belt, and (B) orthogonal to the strike of basin-bounding faults located on the margin and imaged beneath the Coastal Plain. Hypocenters were collapsed using the methodology of Jones and Stewart (1997). For comparison between the un-collapsed and collapsed hypocenter locations see Supplementary Fig. 1. Hypocenters (which are shown as black dots) are projected from 4.99 km on either side of the sections. Seismic events range up to >7 M_L. Dashed white line indicates the 5.2 km/s isovelocity line. The surface location of the major faults (fault abbreviations are as in Fig. 2) and the points of intersection between sections are shown. The location of the sections is indicated in Fig. 2.

Chaochou faults, earthquake hypocenters form a well-defined, sub-horizontal cluster near the basement-cover interface. Nevertheless, in the collapsed data set it is not possible to make a direct correlation between any fault mapped at the surface and the hypocenter data forming this sub-horizontal cluster, although other authors have attempted this with un-collapsed data (e.g., Wu et al., 2003). As the basement-cover interface deepens to the south, however, there is a significant reduction in the number of events (i.e., in sections E-E′ and F-F′) (see also Fig. 5). From approximately the Shuilikeng and Chaochou faults to the east, hypocenters form a moderately east-dipping cluster that locally extends to a depth of more than 20 km. This feature is particularly well developed in sections A-A′, E-E′, and F-F′ (Fig. 4A). Farther east, seismicity is diffuse. This deepening of the seismicity coincides with a marked shallowing of the basement-cover interface (Figs. 4 and 5). An exception to this relationship between the basement-cover interface and the seismicity is a well-defined cluster that begins near the Shuilikeng Fault and extends westward in sections B-B′, C-C′ and G-G′. This cluster (named LuF in Figs. 4 and 5) is related to a series of earthquakes that were observed before, but predominantly after the 1999 Chi-Chi event (Wu et al., 2004) that, in 3D, has a tubular shape, and in which strike-slip focal mechanisms dominate (Wu et al., 2010). Wu et al. (2004) and Lee and Shih (2011) suggest that this seismicity is related to the Luliao Fault.

In the sections perpendicular to the extensional faults imaged offshore southwest Taiwan and beneath the Coastal Plain, the southward deepening of the basement-cover interface is particularly well-defined in sections J-J′ and K-K′ (Fig. 4B). In the sections that cross the Shuilikeng and Chaochou faults (G-G′ through to J-J′) the marked shallowing of the basement-cover interface is also imaged. In sections G-G′ to I-I′, hypocenters form sub-horizontal clusters near the basement-cover interface, although in section H-H′ a weakly developed vertical cluster can also be identified; it extends down to a little over 15 km depth. Section J-J′ displays moderately SSE-dipping, tight to open clusters of hypocenters together with the sub-horizontal events. Together they define an overall deepening of the basement-cover interface with a rugose or step-like geometry. Section K-K′ shows very clearly the SE-deepening of the basement-cover interface and, where it is at its deepest, the almost complete absence of seismicity (Figs. 4B and 5).

Throughout the study area, there is a notable difference between the location of the deformation front and the western limit of the seismicity (as defined by a significant reduction in the number of earthquakes). To demonstrate this, all hypocenters from 0 to 30 km depth are projected onto a map of the surface geology of the Coastal Plain and the Western Foothills within the study area (Fig. 6). In the northern part of the map area the majority of the seismicity is east of the deformation front as defined by the Changhua thrust tip line, whereas southward it locally

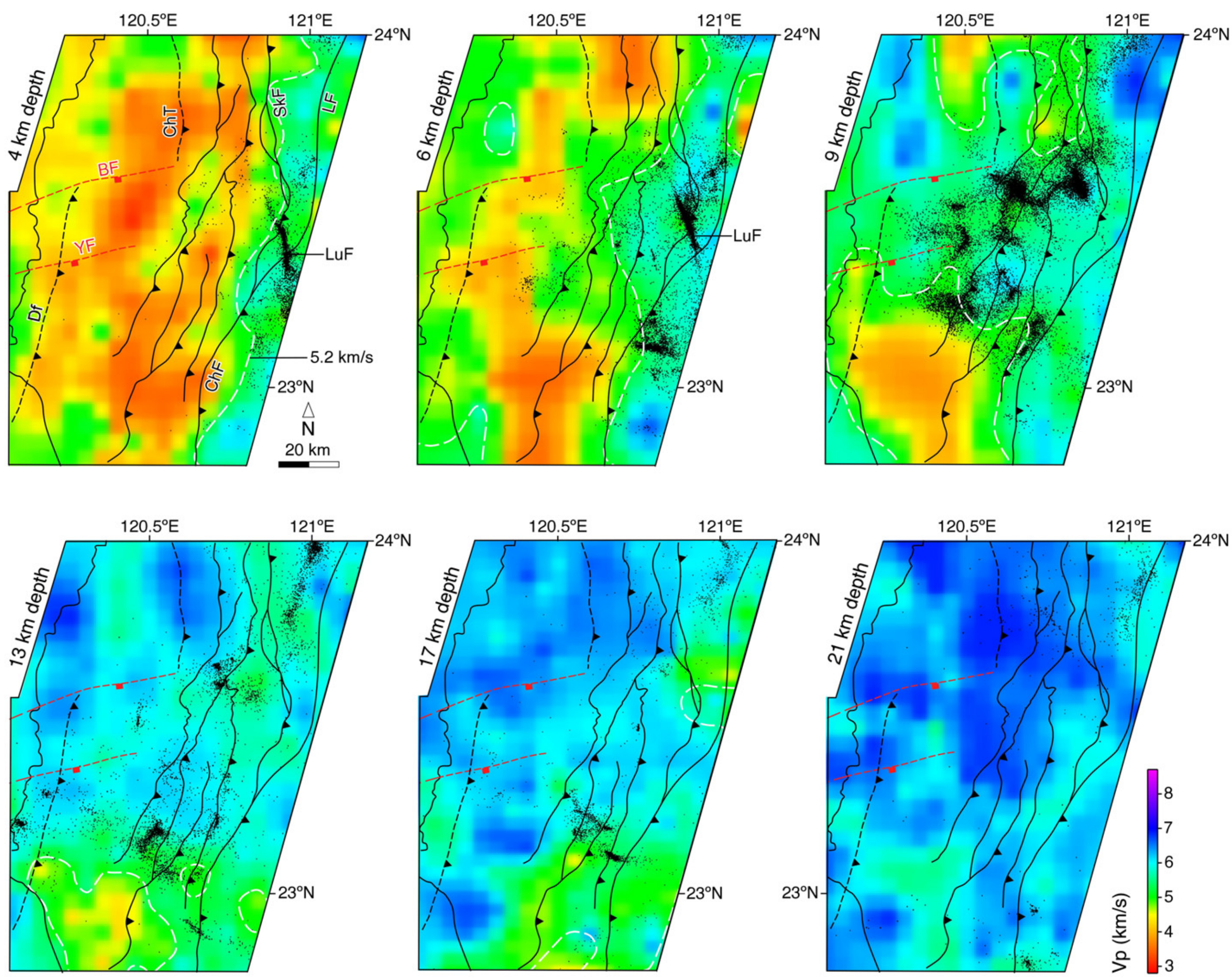

Fig. 5. Horizontal slices through the 3D P-wave velocity model (Wu et al., 2007) and the relocated (Wu et al., 2008) and collapsed seismicity dataset used in this study. The depth intervals are dependent on the vertical resolution of the 3D P-wave velocity model. Hypocenters (shown as black dots) are projected from 0.99 km on either side of the horizontal slices. Seismic events range up to >7 M_L. Dashed white line indicates the 5.2 km/s isovelocity line. Fault abbreviations are as in Fig. 2. Location of the maps is given in Fig. 2.

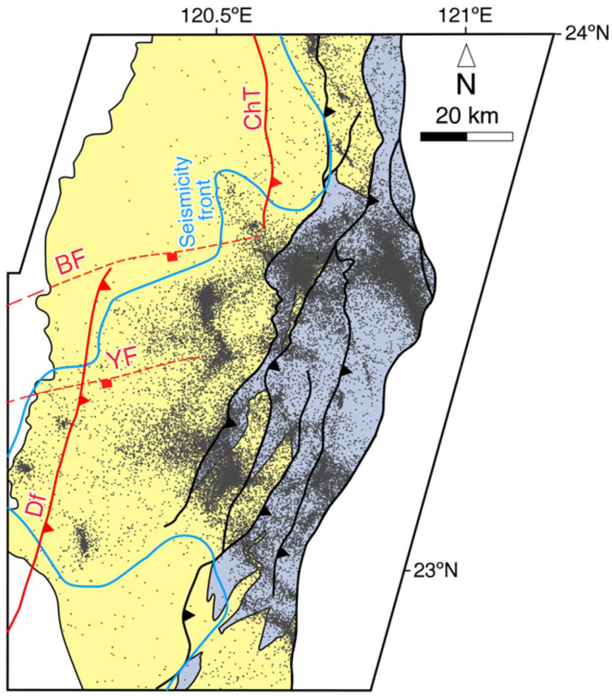

Fig. 6. Geological map of the Coastal Plain and Western Foothills within the study area, and the collapsed earthquake hypocenters from 0 to 30 km depth. The blue line marks the seismicity front that is defined by a marked reduction in the number of earthquakes. Note how the seismicity front does not coincide with the Changhua Thrust tip line nor with the deformation front, in the northern and southwestern parts of the study area, respectively. Colors and location of the map are given in Fig. 2.

extends west of the deformation front as defined by Shyu et al. (2005). In the southwest, where the sedimentary package of the Tainan Basin is thickest, there are also very few events. The distribution of hypocenters suggests that the western limit of the deformation may not coincide everywhere with the deformation front of the mountain belt as it is often interpreted (Ching et al., 2011b; Hsu et al., 2009; Lin and Watts, 2002; Shyu et al., 2005; Yang et al., 2007; Yu et al., 1997).

5. Discussion

5.1. The deep structure of south-central Taiwan

The Eurasian continental margin that is entering into the collision currently taking place in Taiwan has been extensively studied, in particular in the offshore to the southwest (Ding et al., 2008; Eakin et al., 2014; Huang et al., 2004; Lester et al., 2014; Li et al., 2007; Lin et al., 2003; McIntosh et al., 2013; Tang and Zheng, 2010; Yang et al., 2006). This area of the margin comprises the platform (full thickness of the continental crust), the slope (starting at the 200 m bathymetry contour, Figs. 1 and 2), and the continent-ocean transition. On the outer platform to slope areas of the margin Miocene extension resulted in the development of the deep Tainan Basin offshore southwest Taiwan (Figs. 1 and 2) (Ding et al., 2008; Huang et al., 2004; Lester et al., 2014; Li et al., 2007; Lin et al., 2003; Tang and Zheng, 2010; Yang et al., 2006). The Tainan Basin comprises two fault-bound depocentres called the Northern and Southern depressions, separated by a structural high called the Central Uplift (Fig. 7, section X-X′). The thickness of the Oligocene and Miocene sediments in the Tainan Basin offshore reaches up to 6 km, and these are overlain by up to 7 km (in the Southern Depression) of Pliocene to Holocene syn-orogenic sediments (Lin et al., 2003). The Tainan Basin is bound to the north by a system of SSE-dipping extensional faults that have been grouped together and called "B" (Lin et al., 2003) or Meishan (Yang et al., 2007) and Yichu faults (Fig. 2) (Lin et al., 2003). Although there are a number of very different structural interpretations for the extensional fault geometries of the Tainan Basin (e.g., Chen and Yang, 1996; Huang et al., 2004; Lin et al., 2003), the overall regional-scale architecture can be interpreted to project onshore where it appears to be imaged by the step-like geometry of the hypocenter cluster and overall southward deepening of the basement-cover interface in section J-J′ (Fig. 7).

While this rugose geometry of the hypocenter cluster is not well-developed everywhere (in the offshore Lester et al. (2013) and Eakin et al. (2014) have imaged a similar rugose detachment at the basement-cover interface), from the Shuilikeng and Chaochou faults to the west there is nevertheless a well-defined clustering of hypocenters near the basement-cover interface as we define it (Fig. 4). The clustering of hypocenters at the basement-cover interface suggests that it is acting as a detachment surface (Fig. 7), with its western limits coinciding with the seismicity front (as defined in Section 4.2). This, taken together with the rugose nature of the hypocenter cluster imaged in section J-J′ may indicate that the original basement structure of the continental margin (i.e., section X-X′ in Fig. 7) is preserved in the southwestern part of the Taiwan mountain belt. It may also indicate that the extensional fault systems developed on the outer platform to slope maintain at least some of their original extensional displacement in this part of the mountain belt (Fig. 7). However, the development of the Alishan Uplift in the central part of the map area appears to indicate that these faults are locally being reactivated (Alvarez-Marron et al., 2014).

The deep level (≥10 km) of the hypocenter cluster along the basement-cover interface make it difficult to link the geometry of the thrust systems developed at the surface (Alvarez-Marron et al., 2014; Hickman et al., 2002; Lacombe et al., 1999; Mouthereau et al., 2001; Suppe, 1976; Suppe and Namson, 1979) to a detachment at this depth (see Yue et al. (2005) for a discussion of this point). This suggests that there might be a deeper, active level of detachment near the basement-cover interface that is located beneath the basal thrust of the upper thrust system throughout a large part of south-central Taiwan. Both appear to be active at the same time, although seismicity seems to be largely taking place along the deeper of the two.

There is a considerable change in the surface geology across the Shuilikeng, Lishan, and Chaochou faults (Fig. 7) that is clearly expressed in the P-wave velocity and hypocenter data (Figs. 3, 4, and 5). To the west of these faults the deformation is confined to shallow crustal levels, whereas to the east the hypocenter cluster deepens to greater than 20 km depth and coincides with higher P-wave velocity material closer to the surface. In the northern part of the study area, Brown et al. (2012) and Camanni et al. (2014b) suggest that this is related to the uplift of basement rocks between the Shuilikeng and Lishan faults (sections A-A′ in Figs. 4A and 7). With the current data set we can interpret this same process (uplift of basement rocks) to extend southward along the Chaochou Fault, where the sub-horizontal cluster imaged to the west takes on an eastward dip and extends to 20 km or more depth (sections E-E′ and F-F′ in Figs. 4A and 7). In this interpretation the detachment located near the basement-cover interface beneath the Coastal Plain and the Western Foothills ramps down section to merge with the Chaochou Fault that uplift the higher velocity, denser basement rocks in the east to near the surface. This interpretation implies that the Shuilikeng, Lishan, and Chaochou faults are linked together and in some way are rooted into the middle or even lower crust along this east-dipping hypocenter cluster (Fig. 7). This interpretation is in keeping with those of Ching et al. (2011a), Huang and Byrne (2014), Mouthereau et al. (2002), Tang et al. (2011), and Wiltschko et al. (2010) who also interpret the Chaochou fault to be rooted deep in the crust. With the current data set from south-central Taiwan it is not possible, however, to establish that (or even if) this detachment extends eastward into the internal part of the mountain belt, that is beneath the Central Range. The lack of seismicity beneath the internal part

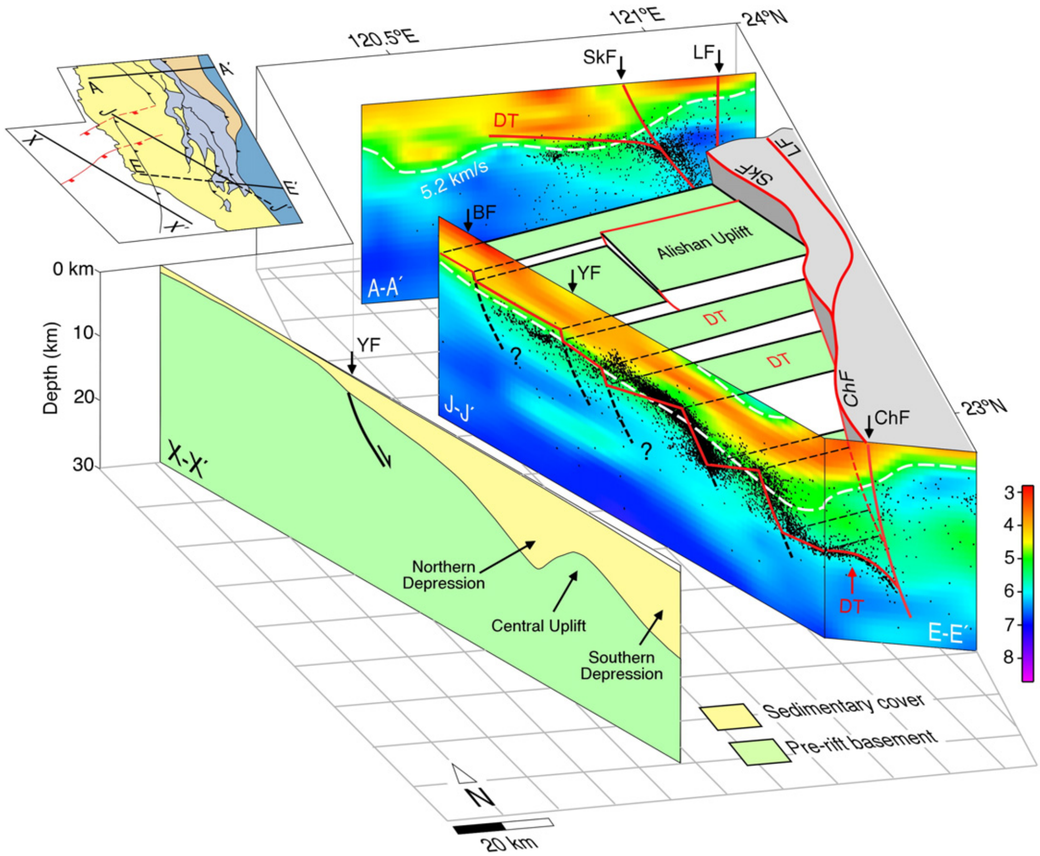

Fig. 7. Schematic block diagram showing the interpreted deep structure beneath the study area. Section X-X′ is drawn using the sedimentary thicknesses offshore southwest Taiwan proposed by Lin et al. (2003). Note how the deepening of the basement shown in section X-X′ can be interpreted to project onshore to section J-J′, where the large-scale structural architecture appears to be preserved. Eastward, the basement shallows across the Shuilikeng and Chaochou faults. The basement cover interface beneath the Coastal Plain and the Western Foothills appears to be acting as an extensive zone of detachment (DT) that, eastward, merges with the deep trace of the Shuilikeng and Chaochou faults. Fault abbreviations are as in Fig. 2.

of the mountain belt may indicate higher temperatures (Wu et al., 1997), and possibly that ductile (e.g., Mouthereau et al., 2009; Yamato et al., 2009) deformation could be taking place in this part of the orogen.

5.2. The influence of basement faults inherited from the Eurasian continental margin on the structural development of south-central Taiwan

One of the basic tenets in the geometric, mechanical, numerical, and analogue modeling of mountain belts is that at shallow depths beneath their flanks there is a through-going, gently-dipping detachment above which a thrust belt develops (e.g., Poblet and Lisle, 2011; Rodgers, 1990). In this model, the sedimentary cover of a continental margin is detached above a basement that is not extensively involved in the deformation (Buiter, 2012; Chapple, 1978; Dahlen et al., 1984; Dahlstrom, 1970; Davis et al., 1983; Fitz-Diaz et al., 2011; Pérez-Estaún et al., 1988, 1994; Price, 1981). While this simplified view of thrust belt architecture is widely accepted, how a rifted continental margin deforms during collision depends to a large degree on its prior morphology, structure, and rheology (e.g., Brown et al., 2011; Butler et al., 2006; Mouthereau et al., 2013; Thomas, 2006). In particular, it is a common feature in a number of thrust belts worldwide, that their structure is variably influenced by the reactivation of extensional faults inherited from the rifted continental margin (e.g., Brown et al., 1999; Butler et al., 1997; Hatcher and Williams, 1986; Laubscher, 1965; Narr and Suppe, 1994; Pérez-Estaún et al., 1997; Rodgers, 1987; Schmidt et al., 1988; Wiltschko and Eastman, 1983; Woodward, 1988). During the structural evolution of a thrust belt, such inherited faults can be fully or partially inverted often resulting in the uplift of basement rocks and in the development of lateral structures in either the footwall or hanging wall (e.g., Bonini et al., 2012; Coward et al., 1991, 1999; De Paola et al., 2006; Di Domenica et al., 2014; Jackson, 1980; Madritsch et al., 2008; Molinaro et al., 2005; Sibson, 1995). In addition, they can localize deformation, causing the development of structures such as buttresses and back-thrusts (e.g., Casciello et al., 2013; de Graciansky et al., 1989; Gillcrist et al., 1987).

The results obtained in this study provide further insights into how basement faults that are inherited from a rifted continental margin may affect the structural development of a thrust belt. They indicate that the along-strike geometry of a detachment, during its early stages of development, if it is located near the basement-cover interface, may be non-planar as it adjusts to the inherited regional-scale geometry of the underlying rifted basement. This type of effect can be seen beneath the Coastal Plain and Western Foothills of south-central Taiwan where the detachment near the basement-cover interface has a rough (rugose) geometry that can be interpreted to be related to the regional-scale rift-related structure found offshore to the southwest. We suggest, therefore, that in thrust belts developed at an angle to a rifted margin, a detachment with a rough, along-strike geometry can be expected to develop. Furthermore, this detachment at the basement-cover interface, such as that described here for south-central Taiwan can be very seismically active. Finally, the local inversion of inherited basement faults can cause lateral structures and basement uplifts. An example of these is in the Alishan Uplift where inversion of rift-related faults that can be traced from the offshore is resulting in basement rocks becoming involved in the deformation (Alvarez-Marron et al., 2014). This interpretation is similar to that of other authors that suggest that pre-existing extensional faults in the Coastal Plain and Western Foothills of south-central Taiwan are being reactivated (e.g., Lacombe and Mouthereau, 2002; Mouthereau and Lacombe, 2006; Mouthereau and Petit, 2003; Mouthereau et al., 2002; Suppe, 1986). Mouthereau and Petit (2003) even interpret seismicity in the southwesternmost part of Taiwan to be related to widespread reactivation of pre-existing extensional faults rather than to deformation taking place near the basement-cover interface as we interpret it.

Our results also show that, in south-central Taiwan, the detachment at the basement-cover interface eastward becomes a ramp into the middle crust along its entire length (i.e., the Shuilikeng–Chaochou fault system). In the hanging wall of this ramp, rocks with a relatively higher P-wave velocity that we interpret to be basement are uplifted. Along the Shuilikeng Fault, this ramp can be interpreted to be the inverted bounding fault of the Hsuehshan Basin (Camanni et al., 2014a,2014b). Southward, the significance of the Chaochou Fault in the context of the rifted margin structure is not clear. Nevertheless, the regional-scale geometry of a detachment at the basement-cover interface that, hinterlandward, becomes a ramp into the underlying basement can be found in many thrust belts worldwide (e.g., Cook et al., 1979a,1979b; Coward, 1983a,1983b; Hatcher and Williams, 1986; Pérez-Estaún et al., 1988). Rocks in the hanging walls of these ramps have commonly experienced middle and lower crustal metamorphic conditions and ductile deformation, indicating that they penetrate to very deep levels in the crust. This also appears to be the case for south-central Taiwan (e.g., Brown et al., 2012; Camanni et al., 2014a,2014b) and may provide a geological explanation for the lack of seismicity beneath the Central Range. Nevertheless, the case of Taiwan indicates that seismic activity can occur well into the middle crust along such a ramp. It also indicates the linkage and coeval deformation (denoted by the seismicity) along the whole length of a curved sole thrust ramping from the middle crust in the hinterland through a rugose detachment near the basement-cover interface in the foreland.

6. Conclusions

The combination of seismic tomography and earthquake hypocenter data presented in this paper helps define the deep structure of the south-central Taiwan mountain belt. In this paper we define a proxy for the basement-cover interface to coincide with a P-wave velocity of 5.2 km/s. These data suggest that in the west, beneath the Coastal Plain and the Western Foothills, the mountain belt is evolving above a southward deepening level of detachment that is illuminated by sub-horizontal clusters of earthquake hypocenters located near this basement-cover interface. This detachment appears to be below the basal thrust of the thrust system mapped at the surface and, in much of south-central Taiwan, the western limit of the seismicity that defines the detachment does not coincide with the deformation front of the thrust system at the surface. Eastward, the detachment at the basement-cover interface joins with an east-dipping hypocenter cluster that is interpreted to form a ramp that extends to greater than 20 km depth, into the middle crust. Above this ramp, basement rocks (P-wave > 5.2 km/s) are uplifted to near the surface, forming a basement culmination beneath the Hsuehshan and Central ranges. The uplift of these basement rocks, together with the juxtaposition of higher metamorphic grade rocks across the Shuilikeng, Lishan and Chaochou faults suggests that these faults form a linked fault system that extends downward into the middle crust at the location of the ramp. Finally, the deep structures that we recognized in south-central Taiwan may provide insights into the influence of basement faults inherited from a rifted continental margin on the structural development of other thrust belts worldwide. In particular, deep-seated inherited basement faults can be shown to determine the geometry of the detachment at the basement-cover interface, as well as the development of basement uplifts and lateral structures.

Supplementary data to this article can be found online at http://dx.doi.org/10.1016/j.tecto.2015.09.016.

Acknowledgments

Discussions with E. Casciello, M.-M. Chen, H.-T. Chu, and A. Pérez-Estaún are acknowledged, as the help of C.-H. Chen and H.-A. Chen in the collapsing of the earthquake hypocenters. The Guest Editor J.-C. Lee, F. Mouthereau, and an anonymous reviewer are thanked for their constructive comments on the paper. The earthquake hypocenter database is available from authors or at http://seismology.gl.ntu.edu.tw/download_04.htm. The P-wave velocity model is available from authors or at http://seismology.gl.ntu.edu.tw/data/02.%203D%20Vp%20VpVs%20model.txt. This research was carried out with the aid of grants by Consejo Superior de Investigaciones Científicas (CSIC) Proyectos Intramurales 2006 301010, Ministerio de Ciencia y InnovaciónCGL2009-11843-BTE and CGL2013-43877-P, and the CSIC predoctoral program Junta para la Ampliación de Estudios (JAE-Predoc). The Generic Mapping Tools (GMT) were used to produce some of the figures.

References

Alvarez-Marron, J., Brown, D., Camanni, G., Wu, Y.M., Kuo-Chen, H., 2014. Structural complexities in a foreland thrust belt inherited from the shelf-slope transition: insights from the Alishan area of Taiwan. Tectonics 33 (7), 1322–1339.

Bertrand, E.A., Unsworth, M.J., Chiang, C.-W., Chen, C.-S., Chen, C.-C., Wu, F.T., Türkoğlu, E., Hsu, H.-L., Hill, G.J., 2009. Magnetotelluric evidence for thick-skinned tectonics in central Taiwan. Geology 37 (8), 711–714.

Bertrand, E.A., Unsworth, M.J., Chiang, C.-W., Chen, C.-S., Chen, C.-C., Wu, F.T., Türkoğlu, E., Hsu, H.-L., Hill, G.J., 2012. Magnetotelluric imaging beneath the Taiwan orogen: an arc–continent collision. J. Geophys. Res. 117 (B1).

Beyssac, O., Simoes, M., Avouac, J.P., Farley, K.A., Chen, Y.-G., Chan, Y.-C., Goffé, B., 2007. Late Cenozoic metamorphic evolution and exhumation of Taiwan. Tectonics 26 (6).

Bonini, M., Sani, F., Antonielli, B., 2012. Basin inversion and contractional reactivation of inherited normal faults: a review based on previous and new experimental models. Tectonophysics 522–523, 55–88.

Brown, D., Alvarez-Marron, J., Perez-Estaun, A., Puchkov, V., Ayala, C., 1999. Basement influence on foreland thrust and fold belt development: an example from the southern Urals. Tectonophysics 308 (4), 459–472.

Brown, D., Ryan, P.D., Afonso, J.C., Boutelier, D., Burg, J.P., Byrne, T., Calvert, A., Cook, F., DeBari, S., Dewey, J.F., Gerya, T.V., Harris, R., Herrington, R., Konstantinovskaya, E., Reston, T., Zagorevski, A., 2011. Arc–continent collision: the making of an orogen. In: Brown, D., Ryan, P.D. (Eds.), Arc–Continent Collision: New York, Springer Berlin Heidelberg, pp. 477–493.

Brown, D., Alvarez-Marron, J., Schimmel, M., Wu, Y.-M., Camanni, G., 2012. The structure and kinematics of the central Taiwan mountain belt derived from geological and seismicity data. Tectonics 31 (5).

Buiter, S.J.H., 2012. A review of brittle compressional wedge models. Tectonophysics 530–531, 1–17.

Butler, R.W.H., Holdsworth, R.E., Lloyd, G.E., 1997. The role of basement reactivation in continental deformation. J. Geol. Soc. 154 (1), 69–71.

Butler, R.W.H., Tavarnelli, E., Grasso, M., 2006. Structural inheritance in mountain belts: an Alpine–Apennine perspective. J. Struct. Geol. 28 (11), 1893–1908.

Byrne, T., Chan, Y.C., Rau, R.J., Lu, C.Y., Lee, Y.H., Wang, Y.J., 2011. The arc–continent collision in Taiwan. In: Brown, D., Ryan, P.D. (Eds.), Arc–Continent Collision: New York, Springer Berlin Heidelberg, pp. 213–245.

Camanni, G., Brown, D., Alvarez-Marron, J., Wu, Y.-M., Chen, H.-A., 2014a. The Shuilikeng fault in the central Taiwan mountain belt. J. Geol. Soc. 171, 117–130.

Camanni, G., Chen, C.-H., Brown, D., Alvarez-Marron, J., Wu, Y.-M., Chen, H.-A., Huang, H.-H., Chu, H.-T., Chen, M.-M., Chang, C.-H., 2014b. Basin inversion in central Taiwan and its importance for seismic hazard. Geology 42 (2), 147–150.

Carena, S., Suppe, J., Kao, H., 2002. Active detachment of Taiwan illuminated by small earthquakes and its control of first-order topography. Geology 30 (10), 935–938.

Casciello, E., Esestime, P., Cesarano, M., Pappone, G., Snidero, M., Vergés, J., 2013. Lower plate geometry controlling the development of a thrust-top basin: the tectonosedimentary evolution of the Ofanto basin (Southern Apennines). J. Geol. Soc. 170 (1), 147–158.

Chapple, W.M., 1978. Mechanics of thin-skinned fold-and-thrust belts. Geol. Soc. Am. Bull. 89 (8), 1189–1198.

Chen, A., Yang, Y.-L., 1996. Lack of compressional overprint on the extensional structure in offshore Tainan and the tectonic implications. Terr. Atmos. Ocean. Sci. 7 (4), 505–522.

Ching, K.-E., Johnson, K.M., Rau, R.-J., Chuang, R.Y., Kuo, L.-C., Leu, P.-L., 2011a. Inferred fault geometry and slip distribution of the 2010 Jiashian, Taiwan, earthquake is consistent with a thick-skinned deformation model. Earth Planet. Sci. Lett. 301 (1–2), 78–86.

Ching, K.-E., Rau, R.-J., Johnson, K.M., Lee, J.-C., Hu, J.-C., 2011b. Present-day kinematics of active mountain building in Taiwan from GPS observations during 1995–2005. J. Geophys. Res. Solid Earth 116 (B9).

Chiu, H.-T., 1975. Miocene stratigraphy and its relation to the Paleogene rocks in west-central Taiwan. Pet. Geol. Taiwan 12, 51–80.

Christensen, N.I., 1989. Reflectivity and seismic properties of the deep continental crust. J. Geophys. Res. Solid Earth 94 (B12), 17793–17804.

Christensen, N.I., Stanley, D., 2003. Seismic velocities and densities of rocks. Int. Handb. Earthq. Eng. Seismol. 81 B, 1587–1593.
Chuang, R.Y., Johnson, K.M., Wu, Y.-M., Ching, K.-E., Kuo, L.-C., 2013. A midcrustal ramp-fault structure beneath the Taiwan tectonic wedge illuminated by the 2013 Nantou earthquake series. Geophys. Res. Lett. 40 (19).
Clark, M.B., Fisher, D.M., Lu, C.-Y., Chen, C.-H., 1993. Kinematic analyses of the Hsüehshan Range Taiwan: a large-scale pop-up structure. Tectonics 12 (1), 205–217.
Cook, F.A., Albaugh, D.S., Brown, L.D., Kaufmann, S., Oliver, J.E., Hatcher Jr., R.D., 1979a. Thin-skinned tectonics in the crystalline southern Appalachians: COCORP seismic-reflection profiling of the Blue Ridge and Piedmont. Geology 7 (12), 563–567.
Cook, F.A., Albaugh, D.S., Brown, L.D., Kaufmann, S., Oliver, J.E., Hatcher Jr., R.D., 1979b. Thin-skinned tectonics in the crystalline southern Appalachians: COCORP seismic-reflection profiling of the Blue Ridge and Piedmont. Geology 7 (12), 563–567.
Coward, M.P., 1983a. Thrust tectonics, thin skinned or thick skinned, and the continuation of thrusts to deep in the crust. J. Struct. Geol. 5 (2), 113–123.
Coward, M.P., 1983b. Thrust tectonics, thin skinned or thick skinned, and the continuation of thrusts to deep in the crust. J. Struct. Geol. 5 (2), 113–123.
Coward, M.P., Gillcrist, R., Trudgill, B., 1991. Extensional structures and their tectonic inversion in the Western Alps. Geol. Soc. Lond., Spec. Publ. 56 (1), 93–112.
Coward, M.P., De Donatis, M., Mazzoli, S., Paltrinieri, W., Wezel, F.-C., 1999. Frontal part of the northern Apennines fold and thrust belt in the Romagna-Marche area (Italy): shallow and deep structural styles. Tectonics 18 (3), 559–574.
Dahlen, F.A., Suppe, J., Davis, D., 1984. Mechanics of fold-and-thrust belts and accretionary wedges: cohesive Coulomb Theory. J. Geophys. Res. 89 (B12), 10087–10101.
Dahlstrom, C.D.A., 1970. Structural geology in the eastern margin of the Canadian rocky mountains. Bull. Can. Petrol. Geol. 18 (3), 332–406.
Davis, D., Suppe, J., Dahlen, F.A., 1983. Mechanics of fold-and-thrust belts and accretionary wedges. J. Geophys. Res. 88 (B2), 1153–1172.
de Graciansky, P.C., Dardeau, G., Lemoine, M., Tricart, P., 1989. The inverted margin of the French Alps and foreland basin inversion. In: Cooper, M.A., Williams, G.D. (Eds.), Inversion Tectonics. Geological Society, London, Special Publications vol. 44, pp. 87–104.
De Paola, N., Mirabella, F., Barchi, M.R., Burchielli, F., 2006. Early orogenic normal faults and their reactivation during thrust belt evolution: the Gubbio Fault case study, Umbria-Marche Apennines (Italy). J. Struct. Geol. 28 (11), 1948–1957.
Di Domenica, A., Bonini, L., Calamita, F., Toscani, G., Galuppo, C., Seno, S., 2014. Analogue modeling of positive inversion tectonics along differently oriented pre-thrusting normal faults: an application to the Central-Northern Apennines of Italy. Geol. Soc. Am. Bull. 126 (7–8), 943–955.
Ding, Z.Y., Yang, Y.Q., Yao, Z.X., Zhang, G.H., 2001. A thin-skinned collisional model for the Taiwan orogeny. Tectonophysics 332 (3), 321–331.
Ding, W.-W., Li, J.-B., Li, M.-B., Qiu, X.-L., Fang, Y.-X., Tang, Y., 2008. A Cenozoic tectono-sedimentary model of the Tainan Basin, the South China Sea: evidence from a multi-channel seismic profile. J. Zhejiang Univ. Sci. A 9 (5), 702–713.
Eakin, D.H., McIntosh, K.D., Van Avendonk, H.J.A., Lavier, L., Lester, R., Liu, C.-S., Lee, C.-S., 2014. Crustal-scale seismic profiles across the Manila subduction zone: the transition from intraoceanic subduction to incipient collision. J. Geophys. Res. Solid Earth 119 (1) (p. 2013JB010395).
Fisher, D.M., Lu, C.-Y., Chu, H.-T., 2002. Taiwan slate belt: insights into the ductile interior of an arc–continent collision. Geol. Soc. Am. Spec. Pap. 358, 93–106.
Fitz-Diaz, E., Hudleston, P., Tolson, G., 2011. Comparison of tectonic styles in the Mexican and Canadian Rocky Mountain Fold–Thrust Belt. Geol. Soc. Lond., Spec. Publ. 349 (1), 149–167.
Gillcrist, R., Coward, M.P., Mugnier, J., 1987. Structural inversion and its controls: examples from the Alpine foreland and the French Alps. Geodin. Acta 1, 5–34.
Gourley, J.R., Byrne, T., Chan, Y.-C., Wu, F., Rau, R.-J., 2007. Fault geometries illuminated from seismicity in central Taiwan: implications for crustal scale structural boundaries in the northern Central Range. Tectonophysics 445 (3–4), 168–185.
Hatcher, R.D., Williams, R.T., 1986. Mechanical model for single thrust sheets. Part I: taxonomy of crystalline thrust sheets and their relationships to the mechanical behavior of orogenic belts. Geol. Soc. Am. Bull. 97 (8), 975–985.
Hickman, J.B., Wiltschko, D.V., Hung, J.-H., Fang, P., Bock, Y., 2002. Structure and evolution of the active fold-and-thrust belt of southwestern Taiwan from global positioning system analysis. Geol. Soc. Am. Spec. Pap. 358, 75–92.
Ho, C.-S., 1986. A synthesis of the geologic evolution of Taiwan. In: Angelier, J., Blanchet, R., Ho, C.-S., Le Pichon, X. (Eds.), Geodynamics of the Eurasia–Philippine Sea Plate Boundary. Tectonophysics vol. 125, pp. 1–16.
Ho, C.-S., 1988. An Introduction to the Geology of Taiwan: Explanatory Text of the Geological Map of Taiwan, Taipei, Central Geological Survey.
Hsu, Y.-J., Yu, S.-B., Simons, M., Kuo, L.-C., Chen, H.-Y., 2009. Interseismic crustal deformation in the Taiwan plate boundary zone revealed by GPS observations, seismicity, and earthquake focal mechanisms. Tectonophysics 479 (1–2), 4–18.
Huang, C., Byrne, T.B., 2014. Tectonic evolution of an active tectonostratigraphic boundary in accretionary wedge: an example from the Tulungwan–Chaochou fault system, southern Taiwan. J. Struct. Geol. 69, 320–333.
Huang, C.-Y., Wu, W.-Y., Chang, C.-P., Tsao, S., Yuan, P.B., Lin, C.-W., Xia, K.-Y., 1997. Tectonic evolution of accretionary prism in the arc–continent collision terrane of Taiwan. Tectonophysics 281 (1–2), 31–51.
Huang, S.-T., Yang, K.-M., Hung, J.-H., Wu, J.-C., Ting, H.-H., Mei, W.-W., Hsu, S.-H., Lee, M., 2004. Deformation front development at the northeast margin of the Tainan Basin, Tainan–Kaohsiung Area, Taiwan. Mar. Geophys. Res. 25 (1–2), 139–156.
Huang, C.-Y., Yuan, P.B., Tsao, S.J., 2006. Temporal and spatial records of active arc–continent collision in Taiwan: a synthesis. Geol. Soc. Am. Bull. 118 (3–4), 274–288.
Huang, H.-H., Wu, Y.-M., Song, X., Chang, C.-H., Lee, S.-J., Chang, T.-M., Hsieh, H.-H., 2014. Joint Vp and Vs tomography of Taiwan: implications for subduction-collision orogeny. Earth Planet. Sci. Lett. 392, 177–191.
Hung, J.-H., Wiltschko, D., Lin, H.-C., Hickman, J., Fang, B., P., and Bock, Y., 1999. Structure and motion of the southwestern Taiwan fold and thrust belt. Terr. Atmos. Ocean. Sci. 10 (3), 543–568.
Jackson, J.A., 1980. Reactivation of basement faults and crustal shortening in orogenic belts. Nature 283 (5745), 343–346.
Jahn, B.-M., Chi, W.-R., Yui, T.-F., 1992. A Late Permian formation of Taiwan (marbles from Chia-Li well No. 1): Pb–Pb isochron and Sr isotope evidence, and its regional geological significance. J. Geol. Soc. China 35, 193–218.
Johnston, J.E., Christensen, N.I., 1992. Shear wave reflectivity, anisotropies, Poisson's ratios, and densities of a southern Appalachian Paleozoic sedimentary sequence. Tectonophysics 210, 1–20.
Johnston, J.E., Christensen, N.I., 1993. Compressional to shear velocity ratios in sedimentary rocks. Int. J. Rock Mech. Min. Sci. Geomech. Abstr. 30 (7), 751–754.
Jones, R.H., Stewart, R.C., 1997. A method for determining significant structures in a cloud of earthquakes. J. Geophys. Res. Solid Earth 102 (B4), 8245–8254.
Kim, K.-H., Chiu, J.-M., Pujol, J., Chen, K.-C., Huang, B.-S., Yeh, Y.-H., Shen, P., 2005. Three-dimensional VP and VS structural models associated with the active subduction and collision tectonics in the Taiwan region. Geophys. J. Int. 162 (1), 204–220.
Kim, K.-H., Chen, K.-C., Wang, J.-H., Chiu, J.-M., 2010. Seismogenic structures of the 1999 M_w 7.6 Chi-Chi, Taiwan, earthquake and its aftershocks. Tectonophysics 489 (1–4), 119–127.
Kuo-Chen, H., Wu, F.T., Roecker, S.W., 2012. Three-dimensional P velocity structures of the lithosphere beneath Taiwan from the analysis of TAIGER and related seismic data sets. J. Geophys. Res. 117 (B6).
Lacombe, O., Mouthereau, F., 2002. Basement-involved shortening and deep detachment tectonics in forelands of orogens: Insights from recent collision belts (Taiwan, Western Alps, Pyrenees). Tectonics 21 (4) (p. 12-11–12-22).
Lacombe, O., Mouthereau, F., Deffontaines, B., Angelier, J., Chu, H.T., Lee, C.T., 1999. Geometry and Quaternary kinematics of fold-and-thrust units of southwestern Taiwan. Tectonics 18 (6), 1198–1223.
Lacombe, O., Mouthereau, F., Angelier, J., Deffontaines, B., 2001. Structural, geodetic and seismological evidence for tectonic escape in SW Taiwan. Tectonophysics 333 (1–2), 323–345.
Laubscher, H.P., 1965. Ein kinematisches Modell der Jurafaltung. Eclogae Geol. Helv. 58, 231–318.
Lee, Y.-H., Shih, Y.-X., 2011. Coseismic displacement, bilateral rupture, and structural characteristics at the southern end of the 1999 Chi-Chi earthquake rupture, central Taiwan. J. Geophys. Res. Solid Earth 116 (B7), B07402.
Lee, J.-C., Angelier, J., Chu, H.-T., 1997. Polyphase history and kinematics of a complex major fault zone in the northern Taiwan mountain belt: the Lishan Fault. Tectonophysics 274 (1–3), 97–115.
Lee, Y.-H., Chen, C.-C., Liu, T.-K., Ho, H.-C., Lu, H.-Y., Lo, W., 2006. Mountain building mechanisms in the Southern Central Range of the Taiwan Orogenic Belt — from accretionary wedge deformation to arc–continental collision. Earth Planet. Sci. Lett. 252 (3–4), 413–422.
Lester, R., McIntosh, K., Van Avendonk, H.J.A., Lavier, L., Liu, C.S., Wang, T.K., 2013. Crustal accretion in the Manila trench accretionary wedge at the transition from subduction to mountain-building in Taiwan. Earth Planet. Sci. Lett. 375, 430–440.
Lester, R., Van Avendonk, H.J.A., McIntosh, K., Lavier, L., Liu, C.S., Wang, T.K., Wu, F., 2014. Rifting and magmatism in the northeastern South China Sea from wide-angle tomography and seismic reflection imaging. J. Geophys. Res. Solid Earth 119 (3), 2305–2323.
Li, C.-F., Zhou, Z., Li, J., Hao, H., Geng, J., 2007. Structures of the northeasternmost South China Sea continental margin and ocean basin: geophysical constraints and tectonic implications. Mar. Geophys. Res. 28 (1), 59–79.
Lin, C.-H., 2007. Tomographic image of crustal structures across the Chelungpu Fault: is the seismogenic layer structure- or depth-dependent? Tectonophysics 443 (3–4), 271–279.
Lin, A.T., Watts, A.B., 2002. Origin of the West Taiwan basin by orogenic loading and flexure of a rifted continental margin. J. Geophys. Res. Solid Earth 107 (B9), 2185.
Lin, A.T., Watts, A.B., Hesselbo, S.P., 2003. Cenozoic stratigraphy and subsidence history of the South China Sea margin in the Taiwan region. Basin Res. 15 (4), 453–478.
Lin, A.T., Liu, C.-S., Lin, C.-C., Schnurle, P., Chen, G.-Y., Liao, W.-Z., Teng, L.S., Chuang, H.-J., Wu, M.-S., 2008. Tectonic features associated with the overriding of an accretionary wedge on top of a rifted continental margin: an example from Taiwan. Mar. Geol. 255 (3–4), 186–203.
Madritsch, H., Schmid, S.M., Fabbri, O., 2008. Interactions between thin- and thick-skinned tectonics at the northwestern front of the Jura fold-and-thrust belt (eastern France). Tectonics 27 (5).
Malavieille, J., Trullenque, G., 2009. Consequences of continental subduction on forearc basin and accretionary wedge deformation in SE Taiwan: insights from analogue modeling. Tectonophysics 466 (3–4), 377–394.
McIntosh, K., van Avendonk, H., Lavier, L., Lester, W.R., Eakin, D., Wu, F., Liu, C.-S., Lee, C.-S., 2013. Inversion of a hyper-extended rifted margin in the southern Central Range of Taiwan. Geology 41, 871–874.
Mesalles, L., Mouthereau, F., Bernet, M., Chang, C.-P., Lin, A.T., Fillon, C., Sengelen, X., 2014. From submarine continental accretion to arc–continent orogenic evolution: the thermal record in southern Taiwan. Geology 42, 907–910.
Molinaro, M., Leturmy, P., Guezou, J.C., Frizon de Lamotte, D., Eshraghi, S.A., 2005. The structure and kinematics of the southeastern Zagros fold-thrust belt, Iran: from thin-skinned to thick-skinned tectonics. Tectonics 24 (3).
Mouthereau, F., Lacombe, O., 2006. Inversion of the Paleogene Chinese continental margin and thick-skinned deformation in the Western Foreland of Taiwan. J. Struct. Geol. 28 (11), 1977–1993.

Mouthereau, F., Petit, C., 2003. Rheology and strength of the Eurasian continental lithosphere in the foreland of the Taiwan collision belt: constraints from seismicity, flexure, and structural styles. J. Geophys. Res. Solid Earth 108 (B11).
Mouthereau, F., Lacombe, O., Deffontaines, B., Angelier, J., Brusset, S., 2001. Deformation history of the southwestern Taiwan foreland thrust belt: insights from tectono-sedimentary analyses and balanced cross-sections. Tectonophysics 333 (1–2), 293–318.
Mouthereau, F., Deffontaines, B., Lacombe, O., Angelier, J., 2002. Variations along the strike of the Taiwan thrust belt: basement control on structural style, wedge geometry, and kinematics. In: Byrne, T., Liu, C.S. (Eds.), Geology and Geophysics of an Arc–Continent Collision, Taiwan. Geological Society of America Special Papers vol. 358, pp. 31–54.
Mouthereau, F., Fillon, C., Ma, K.-F., 2009. Distribution of strain rates in the Taiwan orogenic wedge. Earth Planet. Sci. Lett. 284, 361–385.
Mouthereau, F., Watts, A.B., Burov, E., 2013. Structure of orogenic belts controlled by lithosphere age. Nat. Geosci. 6, 785–789.
Narr, W., Suppe, J., 1994. Kinematics of basement-involved compressive structures. Am. J. Sci. 294 (7), 802–860.
Pérez-Estaún, A., Bastida, F., Alonso, J.L., Marquinez, J., Aller, J., Alvarez-Marron, J., Marcos, A., Pulgar, J.A., 1988. A thin-skinned tectonics model for an arcuate fold and thrust belt: the Cantabrian Zone (Variscan Ibero–Armorican Arc). Tectonics 7 (3), 517–537.
Pérez-Estaún, A., Pulgar, J.A., Banda, E., Alvarez-Marrón, J., 1994. Crustal structure of the external variscides in northwest Spain from deep seismic reflection profiling. Tectonophysics 232 (1–4), 91–118.
Pérez-Estaún, A., Alvarez-Marrón, J., Brown, D., Puchkov, V., Gorozhanina, Y., Baryshev, V., 1997. Along-strike structural variations in the foreland thrust and fold belt of the southern Urals. Tectonophysics 276 (1–4), 265–280.
Poblet, J., Lisle, R.J., 2011. Kinematic evolution and structural styles of fold-and-thrust belts. In: Poblet, J., Lisle, R.J. (Eds.), Kinematic Evolution and Structural Styles of Fold-and-Thrust Belts. Geological Society, London, Special Publications vol. 349, pp. 1–24.
Price, R.A., 1981. The Cordilleran foreland thrust and fold belt in the southern Canadian Rocky Mountains. In: McClay, K., Price, N.J. (Eds.), Thrust and Nappe Tectonics. Geological Society, London, Special Publications vol. 9, pp. 427–448.
Rau, R.-J., Wu, F.T., 1995. Tomographic imaging of lithospheric structures under Taiwan. Earth Planet. Sci. Lett. 133 (3–4), 517–532.
Rodgers, J., 1987. Chains of basement uplifts within cratons marginal to orogenic belts. Am. J. Sci. 287 (7), 661–692.
Rodgers, J., 1990. Fold-and-thrust belts in sedimentary rocks. Part 1, typical examples. Am. J. Sci. 290 (4), 321–359.
Rodriguez-Roa, F.A., Wiltschko, D.V., 2010. Thrust belt architecture of the central and southern Western Foothills of Taiwan. Geol. Soc. Lond., Spec. Publ. 348 (1), 137–168.
Sakaguchi, A., Yanagihara, A., Ujiie, K., Tanaka, H., Kameyama, M., 2007. Thermal maturity of a fold–thrust belt based on vitrinite reflectance analysis in the Western Foothills complex, western Taiwan. Tectonophysics 443 (3–4), 220–232.
Schmidt, C.J., O'Neill, J.M., Brandon, W.C., 1988. Influence of Rocky Mountain foreland uplifts on the development of the frontal fold and thrust belt, southwestern Montana. In: Schmidt, C.J., Perry, W.J. (Eds.), Interaction of the Rocky Mountain Foreland and the Cordilleran Thrust Belt. Geological Society of America Memoir vol. 171, pp. 171–201.
Shaw, C.-L., 1996. Stratigraphic correlation and isopach maps of the Western Taiwan Basin. Terr. Atmos. Ocean. Sci. 7, 333–360.
Shyu, J.B.H., Sieh, K., Chen, Y.-G., Liu, C.-S., 2005. Neotectonic architecture of Taiwan and its implications for future large earthquakes. J. Geophys. Res. Solid Earth 110 (B8), B08402.
Sibson, R.H., 1995. Selective fault reactivation during basin inversion: potential for fluid redistribution through fault-valve action. In: Buchanan, J.G., Buchanan, P.G. (Eds.), Basin Inversion. Geological Society, London, Special Publications vol. 88, pp. 3–19.
Sibuet, J.-C., Hsu, S.-K., 2004. How was Taiwan created? Tectonophysics 379 (1–4), 159–181.
Simoes, M., Avouac, J.P., Beyssac, O., Goffé, B., Farley, K.A., Chen, Y.-G., 2007. Mountain building in Taiwan: a thermokinematic model. J. Geophys. Res. Solid Earth 112 (B11).
Simoes, M., Beyssac, O., Chen, Y.-G., 2012. Late Cenozoic metamorphism and mountain building in Taiwan: a review. J. Asian Earth Sci. 46, 92–119.
Stanley, R.S., Hill, L.B., Chang, H.C., Hu, H.N., 1981. A transect through the metamorphic core of the central mountains, southern Taiwan. Mem. Geol. Soc. China 4, 443–473.
Suppe, J., 1976. Decollement folding in southwestern Taiwan. Pet. Geol. Taiwan 13, 25–35.
Suppe, J., 1980. A retrodeformable cross section of northern Taiwan. Proc. Geol. Soc. China 23, 46–55.
Suppe, J., 1981. Mechanics of mountain building and metamorphism in Taiwan. Mem. Geol. Soc. China 4, 67–89.
Suppe, J., 1984. Kinematics of arc–continent collision, flipping of subduction, and back-arc spreading near Taiwan. Mem. Geol. Soc. China 6, 21–33.
Suppe, J., 1986. Reactivated normal faults in the Western Taiwan fold-and-thrust belt. Mem. Geol. Soc. China 7, 187–200.
Suppe, J., Namson, J., 1979. Fault-bend origin of frontal folds of the western Taiwan fold-and-thrust belt. Pet. Geol. Taiwan 16, 1–18.
Tang, Q., Zheng, C., 2010. Seismic velocity structure and improved seismic image of the southern depression of the Tainan Basin from pre-stack depth migration. Terr. Atmos. Ocean. Sci. 21 (5), 807–816.
Tang, C.-C., Zhu, L., Chen, C.-H., Teng, T.-L., 2011. Significant crustal structural variation across the Chaochou Fault, southern Taiwan: new tectonic implications for convergent plate boundary. J. Asian Earth Sci. 41 (6), 564–570.
Teng, L.S., 1990. Geotectonic evolution of late Cenozoic arc–continent collision in Taiwan. Tectonophysics 183 (1–4), 57–76.
Teng, L.S., Lin, A.T., 2004. Cenozoic tectonics of the China continental margin: insights from Taiwan. In: Malpas, J., Fletcher, C.J.N., Ali, J.R., Aitchison, J.C. (Eds.), Aspects of the Tectonic Evolution of China. Geological Society, London, Special Publications vol. 226, pp. 313–332.
Thomas, W.A., 2006. Tectonic inheritance at a continental margin. GSA Today 16 (2), 4–11.
Tillman, K.S., Byrne, T.B., 1995. Kinematic analysis of the Taiwan Slate Belt. Tectonics 14 (2), 322–341.
Van Avendonk, H.J.A., Kuo-Chen, H., McIntosh, K.D., Lavier, L.L., Okaya, D.A., Wu, F.T., Wang, C.Y., Liu, C.S., 2014. Deep crustal structure of an arc–continent collision: constraints from seismic traveltimes in central Taiwan and the Philippine Sea. J. Geophys. Res. Solid Earth 119.
Wiltschko, D., Eastman, D., 1983. Role of basement warps and faults in localizing thrust fault ramps. In: Hatcher, R.D., Williams, H., Zietz, I. (Eds.), Contributions to the Tectonics and Geophysics of Mountain Chains. Geological Society of America Memoir vol. 158, pp. 177–190.
Wiltschko, D., Hassler, L., Hung, J.-H., Liao, H.-S., 2010. From accretion to collision: motion and evolution of the Chaochou Fault, southern Taiwan. Tectonics 29 (2).
Woodward, N.B., 1988. Primary and secondary basement controls on thrust sheet geometries. In: Schmidt, C.J., Perry, W.J. (Eds.), Interaction of the Rocky Mountain Foreland and the Cordilleran Thrust Belt. Geological Society of America Memoir vol. 171, pp. 353–366.
Wu, F.T., Rau, R.-J., Salzberg, D., 1997. Taiwan orogeny: thin-skinned or lithospheric collision? Tectonophysics 274 (1–3), 191–220.
Wu, Y.M., Chang, C.H., Hsiao, N.-C., Wu, F., 2003. Relocation of the 1998 Rueyli, Taiwan, earthquake sequence using three-dimension velocity structure with stations corrections. Terr. Atmos. Ocean. Sci. 14 (4), 421–430.
Wu, F.T., Chang, C.-H., Wu, Y.-M., 2004. Precisely relocated hypocentres, focal mechanisms and active orogeny in Central Taiwan. In: Malpas, J., Fletcher, C.J.N., Ali, J.R., Aitchison, J.C. (Eds.), Aspects of the Tectonic Evolution of China. Geological Society, London, Special Publications vol. 226, pp. 333–354.
Wu, Y.-M., Chang, C.-H., Zhao, L., Shyu, J.B.H., Chen, Y.-G., Sieh, K., Avouac, J.-P., 2007. Seismic tomography of Taiwan: improved constraints from a dense network of strong motion stations. J. Geophys. Res. Solid Earth 112 (B8).
Wu, Y.-M., Chang, C.-H., Zhao, L., Teng, T.L., Nakamura, M., 2008. A comprehensive relocation of earthquakes in Taiwan from 1991 to 2005. Bull. Seismol. Soc. Am. 98 (3), 1471–1481.
Wu, Y.-M., Hsu, Y.-J., Chang, C.-H., Teng, L.S.-y., Nakamura, M., 2010. Temporal and spatial variation of stress field in Taiwan from 1991 to 2007: insights from comprehensive first motion focal mechanism catalog. Earth Planet. Sci. Lett. 298 (3–4), 306–316.
Wu, S.-K., Chi, W.-C., Hsu, S.-M., Ke, C.-C., Wang, Y., 2013. Shallow crustal thermal structures of central Taiwan Foothills Region. Terr. Atmos. Ocean. Sci. 24 (4), 659–707.
Wu, F.T., Kuo-Chen, H., McIntosh, K.D., 2014. Subsurface imaging, TAIGER experiments and tectonic models of Taiwan. J. Asian Earth Sci. 90, 173–208.
Yamato, P., Mouthereau, F., Burov, E., 2009. Taiwan mountain building: insights from 2-D thermomechanical modelling of a rheologically stratified lithosphere. Geophys. J. Int. 176, 307–326.
Yang, K.-M., Huang, S.-T., Wu, J.-C., Ting, H.-H., Mei, W.-W., 2006. Review and new insights on foreland tectonics in western Taiwan. Int. Geol. Rev. 48 (10), 910–941.
Yang, C.-C.B., Chen, W.-S., Wu, L.-C., Lin, C.-W., 2007. Active deformation front delineated by drainage pattern analysis and vertical movement rates, southwestern Coastal Plain of Taiwan. J. Asian Earth Sci. 31 (3), 251–264.
Yeh, Y.-C., Hsu, S.-K., Doo, W.-B., Sibuet, J.-C., Liu, C.-S., Lee, C.-S., 2012. Crustal features of the northeastern South China Sea: insights from seismic and magnetic interpretations. Mar. Geophys. Res. 33 (4), 307–326.
Yu, S.-B., Chen, H.-Y., Kuo, L.-C., 1997. Velocity field of GPS stations in the Taiwan area. Tectonophysics 274 (1–3), 41–59.
Yue, L.-F., Suppe, J., Hung, J.-H., 2005. Structural geology of a classic thrust belt earthquake: the 1999 Chi-Chi earthquake Taiwan (Mw = 7.6). J. Struct. Geol. 27 (11), 2058–2083.
Zhou, D., Yu, H.-S., Xu, H.-H., Shi, X.-B., Chou, Y.-W., 2003. Modeling of thermo-rheological structure of lithosphere under the foreland basin and mountain belt of Taiwan. Tectonophysics 374 (3–4), 115–134.